High-resolution spectroscopy using a frequency magnifier

Yoshitomo Okawachi[1], Reza Salem[1], Mark A. Foster[1], Amy C. Turner-Foster[2], Michal Lipson[2], and Alexander L. Gaeta[1]

[1]*School of Applied and Engineering Physics, Cornell University, Ithaca, NY 14853*
[2]*School of Electrical and Computer Engineering, Cornell University, Ithaca, NY 14853*
a.gaeta@cornell.edu

Abstract: We experimentally demonstrate a spectral magnifier using an imaging system with two time-lenses based on four-wave mixing in a Si nanowaveguide. We achieve a magnification factor of 105 with a frequency resolution of 1 GHz. The system offers potential as a tool for single-shot, high resolution spectral measurements.

OCIS codes: (190.4380) Nonlinear optics, four-wave mixing; (190.4390) Nonlinear optics, integrated optics; (300.1030) Absorption; (320.7100); (070.6020) Continuous optical signal processing.

References and links

1. B. H. Kolner and M. Nazarathy, "Temporal imaging with a time lens," Opt. Lett. **14,** 630–632 (1989).
2. B. H. Kolner, "Space-time duality and the theory of temporal imaging," IEEE J. Quantum Electron. **30,** 1951–1963 (1994).
3. J. van Howe and C. Xu, "Ultrafast optical signal processing based upon space-time dualities," J. Lightwave Technol. **24,** 2649–2662 (2006).
4. L. Kh. Mouradian, F. Louradour, V. Messager, A. Barthélémy, and C. Froehly, "Spectro-temporal imaging of femtosecond events," IEEE J. Quantum Electron. **36,** 795–801 (2000).
5. C. V. Bennett and B. H. Kolner, "Principles of parametric temporal imaging Part I: System configurations," IEEE J. Quantum Electron. **36,** 430–437 (2000).
6. R. Salem, M. A. Foster, A. C. Turner, D. F. Geraghty, M. Lipson, and A. L. Gaeta, "Optical time lens based on four-wave mixing on a silicon chip," Opt. Lett. **33,** 1047–1049 (2008).
7. M. T. Kauffman, W. C. Banyai, A. A. Godil, and D. M. Bloom, "Time-to-frequency converter for measuring picosecond optical pulses," Appl. Phys. Lett. **64,** 270–272 (1994).
8. N. K. Berger, B. Levit, S. Atkins, and B. Fischer, "Time-lens-based spectral analysis of optical pulses by electrooptic phase modulation," Electron. Lett. **36,** 1644–1646 (2000).
9. J. Azaña, N. K. Berger, B. Levit, and B. Fischer, "Spectro-temporal imaging of optical pulses with a single time lens," IEEE Photon. Technol. Lett. **16,** 882–884 (2004).
10. T. Mansuryan, A. Zeytunyan, M. Kalashyan, G. Yesayan, L. Mouradian, F. Louradour, and A. Barthélémy, "Parabolic temporal lensing and spectrotemporal imaging: a femtosecond optical oscilloscope," J. Opt. Soc. Am. B **25,** A101–A110 (2008).
11. M. A. Foster, R. Salem, D. F. Geraghty, A. C. Turner-Foster, M. Lipson, and A. L. Gaeta, "Silicon-chip-based ultrafast optical oscilloscope," Nature, **456,** 81–84 (2008).
12. C. V. Bennett, R. P. Scott, and B. H. Kolner, "Temporal magnification and reversal of 100 Gb/s optical data with an upconversion time microscope," Appl. Phys. Lett. **65,** 2513–2515 (1994).
13. C. V. Bennett and B. H. Kolner, "Upconversion time microscope demonstrating 103x magnification of femtosecond waveforms," Opt. Lett. **24,** 783–785 (1999).
14. A. W. Lohmann and D. Mendlovic, "Temporal filtering with time lenses," Appl. Opt. **31,** 6212–6219 (1992).
15. P. J. Almeida, P. Petropoulos, B. C. Thomsen, M. Ibsen, and D. J. Richardson, "All-optical packet compression based on time-to-wavelength conversion," IEEE Photon. Technol. Lett. **16,** 1688–1690 (2004).
16. T. Sakano, K. Uchiyama, I. Shake, T. Morioka, and K. Hagimoto, "Large-dispersion-tolerance optical signal transmission system based on temporal imaging," Opt. Lett. **27,** 583–585 (2002).

#107440 - $15.00 USD Received 10 Feb 2009; revised 20 Mar 2009; accepted 20 Mar 2009; published 25 Mar 2009

17. M. Nakazawa, T. Hirooka, F. Futami, and S. Watanabe, "Ideal distortion-free transmission using optical Fourier transformation and Fourier transform-limited optical pulses," IEEE Photon. Technol. Lett. **16,** 1059–1061 (2004).
18. V. Torres-Company, J. Lancis, and P. Andrés, "Spectral imaging system for scaling the power spectrum of optical waveforms," Opt. Lett. **32,** 2849–2851 (2007).
19. A. Papoulis, "Dual optical systems," J. Opt. Soc. Am. **58** 653–654 (1968).
20. M. A. Foster, A. C. Turner, R. Salem, M. Lipson, and A. L. Gaeta, "Broad-band continuous-wave parametric wavelength conversion in silicon nanowaveguides," Opt. Express **15,** 12949–12958 (2007).
21. F. Vestin, K. Nilsson, and P.-E. Bengtsson, "Validation of a rotational coherent anti-Stokes Raman spectroscopy model for cabon dioxide using high-resolution detection in the temperature range 294-1143K," Appl. Opt. **47,** 1893–1901 (2008).
22. K. A. Vereschagin, V. V. Smirnov, O, M. Stel'makh, V. I. Fabelinsky, W. Clauss, D. N. Klimenko, M. Oschwald, and A. K. Vereschagin, "Single-shot high resolution dual-broadband interferometric lineshape spectroscopy," J. Raman Spectrosc. **36,** 134–138 (2005).
23. M. F. DeCamp and A. Tokmakoff, "Single-shot two-dimensional spectrometer," Opt. Lett. **31,** 113–115 (2006).
24. J. Brendenbeck, J. Helbing, R. Behrendt, C. Renner, L. Morodor, J. Wachtveitl, and P. Hamm, "2D-IR spectroscopy: snapshots of the nonlinear equilibrium ensemble during the picosecond confirmation transmission of a small peptide," J. Phys. Chem. B **107,** 8654–8660 (2003).
25. H. R. Fetterman, P. E. Tannenwald, C. D. Parker, J. Melngailis, and R. C. Williamson, "Real-time spectral analysis of far-infrared laser pulses using a SAW dispersive delay line," Appl. Phys. Lett. **34,** 123–125 (1979).
26. Y. C. Tong, L. Y. Chan, and H. K. Tsang, "Fibre dispersion or pulse spectrum measurement using a sampling oscilloscope," Electron. Lett. **33** 983–985 (1997).
27. P. V. Kelkar, F. Coppinger, A. S. Bhushan, and B. Jalali, "Time-domain optical sensing," Electron. Lett. **35,** 1661–1662 (1999).
28. S. T. Sanders, "Wavelength-agile fiber laser using group-velocity dispersion of pulsed super-continua and application to broadband absorption spectroscopy," Appl. Phys. B **75,** 799–802 (2002).
29. J. Hult, R. S. Watt, and C. F. Kaminski, "High bandwidth absorption spectroscopy with a dispersed supercontinuum source," Opt. Express **15,** 11385–11395 (2007).
30. J. Chou, D. R. Solli, and B. Jalali, "Real-time spectroscopy with subgigahertz resolution using amplified dispersive Fourier transformation," Appl. Phys. Lett. **92,** 11102 (2008).
31. V. Torres-Company, J. Lancis, and P. Andrés, "Incoherent frequency-to-time mapping: application to incoherent pulse shaping," J. Opt. Soc. Am. A **24,** 888–894 (2007).
32. A. C. Turner, C. Manolatou, B. S. Schmidt, M. Lipson, M. A. Foster, J. E. Sharping, and A. L. Gaeta, "Tailored anomalous group-velocity dispersion in silicon channel waveguides," Opt. Express **14,** 4357–4362 (2006).
33. M. A. Foster, A. C. Turner, J. E. Sharping, B. S. Schmidt, M. Lipson, and A. L. Gaeta, "Broad-band optical parametric gain on a silicon photonic chip," Nature **441,** 960–963 (2006).

1. Introduction

Optical time-lens-based imaging systems have drawn significant interest in applications involving high-speed signal processing. The time-lens takes advantage of the space-time duality of electromagnetic waves [1, 2, 3, 4, 5, 6, 7, 8, 9, 10, 11, 12, 13, 14, 15, 16, 17, 18], where diffractive propagation in the spatial domain has an analog in the temporal domain in the form of dispersive propagation. A time-lens is implemented by applying a quadratic phase shift to the input waveform in the time-domain. Techniques for generating this temporal phase shift include using an electro-optical phase modulator (EOPM) [2], cross-phase modulation (XPM) [4], $\chi^{(2)}$ parametric processes [5], and four-wave mixing (FWM) [6]. Parametric nonlinear optical processes utilize chirped pump pulses and transfer the phase shift to the input signal. This technique allows for much larger phase shifts compared to an EOPM. In addition, the FWM process allows the pump, input signal, and output signal to be at nearby wavelengths, which simplifies the system and allows for easier detection.

The optical time-lens has been used primarily as a tool for characterizing or manipulating temporal features of an optical signal. Applications include spectro-temporal imaging [4, 7, 8, 9, 10, 11], temporal magnification [6, 12, 13], temporal filtering [14], packet compression [15], and signal transmission [16, 17]. In addition, a time-lens can be used to characterize and manipulate frequency features of optical signals. Spectral imaging has been theoretically investigated [18], and a spectral magnification factor of 11 is predicted. This imaging system takes advantage of the duality between the time-lens and temporal dispersion [9, 18, 19], in

#107440 - $15.00 USD Received 10 Feb 2009; revised 20 Mar 2009; accepted 20 Mar 2009; published 25 Mar 2009

which the temporal dispersion is produced by applying the quadratic phase shift in the frequency domain using a dispersive element, analogous to applying the quadratic phase shift in the time-domain.

In this paper, we demonstrate a technique for frequency magnification using a time-lens-based spectral imaging system. Our system consists of two time-lenses based on FWM in a silicon waveguide [20] separated by a dispersive element. We experimentally demonstrate 105× spectral magnification of a single absorption line in acetylene (C_2H_2). Potential applications of the imaging system include single-shot, high-resolution spectral characterization of molecular transitions and transient and nonequilibrium behavior [21, 22, 23, 24].

2. Theory

Time-lens-based imaging systems utilize the analogy between diffractive propagation in the spatial domain and dispersive propagation in the time domain [2]. Paraxial diffraction is analogous to second-order dispersion in the time domain, and the quadratic phase shift imparted in the spatial domain for a spatial lens is analogous to the quadratic phase shift imparted in the time domain for a time-lens. Such an imaging system can be analyzed by solving the propagation equation, where the dispersion operator can be expressed as $G(\omega) = \exp(-i\beta_2\omega^2 L/2)$, where β_2 is the group-velocity dispersion (GVD), and L is the length of the dispersive path. In a FWM-based time-lens, the quadratic phase shift is imparted on the input through interactions with a chirped pump pulse, and the time-lens operator can be expressed as $\tilde{H}(\tau) = \exp(i\tau^2/{\beta_2}^{(p)}L^{(p)})$, where ${\beta_2}^{(p)}$ is the GVD and $L^{(p)}$ is the length of the dispersive path through which the pump pulse propagates.

Recently, a FWM-based time-lens has been used to demonstrate temporal magnification [6]. This imaging system can be modeled as two lengths of dispersion separated by a FWM time-lens [Fig. 1(a)]. By solving the propagation equation, we obtain the lens equation for temporal magnification,

$$\frac{1}{\phi_1''} - \frac{1}{\phi_2''} = \frac{2}{\phi_p''}, \tag{1}$$

where $\phi_1'' = {\beta_2}^{(1)}L^{(1)}$ and $\phi_2'' = {\beta_2}^{(2)}L^{(2)}$ are the group-delay dispersion (GDD) parameters before and after the time-lens, and $\phi_p'' = {\beta_2}^{(p)}L^{(p)}$ is the GDD imparted on the pump pulse. The magnification is given by $M = \phi_2''/\phi_1''$.

The imaging system for spectral magnification consists of two FWM time-lenses separated by two lengths of dispersion, each with a length that corresponds to the focal length of the respective time-lenses. The first time-lens and the length of dispersion provide frequency-to-time conversion, and the second dispersion length and the time-lens provide time-to-frequency conversion. The imaging system can be separated into three stages. The spectral amplitude after the first time-lens is given by

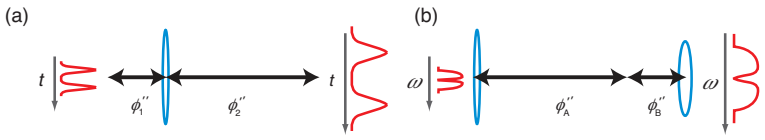

Fig. 1. (a) Single time-lens temporal imaging system. The temporal magnification factor is given by the ratio of the image and object group delay parameters ϕ_2''/ϕ_1''. (b) Two time-lens spectral imaging system. The spectral magnification ratio is $-\phi_A''/\phi_B''$, which corresponds to the ratio of the focal length of the time lenses.

#107440 - $15.00 USD Received 10 Feb 2009; revised 20 Mar 2009; accepted 20 Mar 2009; published 25 Mar 2009

$$A_1(\omega) = \mathscr{F}\left\{\tilde{A}^*_{in}(\tau)\tilde{H}_A(\tau)\right\}, \tag{2}$$

where $\tilde{H}_A(\tau)$ is the first time-lens operator, $\tilde{A}_{in}(\tau)$ is the input field amplitude, and the complex conjugate of the input is inherent to the FWM process. Next, the signal propagates through two GDD lengths, and the corresponding spectral amplitude is

$$A_2(\omega) = \mathscr{F}\left\{\tilde{A}^*_{in}(\tau)\tilde{H}_A(\tau)\right\} G_A(\omega)G_B(\omega), \tag{3}$$

where $G_A(\omega)$ and $G_B(\omega)$ are the operators associated with the first and second dispersive elements. Finally, the signal propagates through the second time lens, and the output spectral amplitude is

$$A_{out}(\omega) = \mathscr{F}\left\{\left(\left[\tilde{A}^*_{in}(\tau)\tilde{H}_A(\tau)\right] \otimes \mathscr{F}^{-1}\left[G_A(\omega)G_B(\omega)\right]\right)^* \tilde{H}_B(\tau)\right\}. \tag{4}$$

The imaging condition for spectral magnification is satisfied by canceling the quadratic phase shift, which distorts the signal, and is achieved by setting the quadratic phase term in Eq. (4) equal to zero. The lens equation for spectral magnification is

$$\frac{\phi_p''^{(B)}}{2} - \frac{\phi_p''^{(A)}}{2} = \phi_A'' + \phi_B'', \tag{5}$$

where $\phi_A'' = \beta_2{}^{(A)}L^{(A)}$ and $\phi_B'' = \beta_2{}^{(B)}L^{(B)}$ are the GDD parameters for the elements between the two time-lenses, and $\phi_p''^{(A)} = \beta_2^{(pA)}L^{(pA)}$ and $\phi_p''^{(B)} = \beta_2^{(pB)}L^{(pB)}$ are the GDD imparted on the pump pulses in the first and second time-lenses. The magnification for this spectral imaging system is given by $M = \phi_p''^{(A)}/\phi_p''^{(B)} = -\phi_A''/\phi_B''$.

Frequency-to-time conversion has been previously demonstrated using a single dispersive element and has been utilized as a tool for pulse spectrum characterization [25, 26] and optical sensing [27, 28, 29, 30]. For such a system, the spectral information is mapped to the time domain through dispersive broadening, so that larger amounts of dispersion are required to resolve smaller frequency features. One major advantage to using the time-lens-based scheme demonstrated here is that the length of the dispersive link required for the frequency-to-time conversion is greatly reduced, which allows for a significant reduction of propagation losses. The time-lens operator adds a frequency chirp to the input signal, which results in an enhancement in the spectral width of the input, thus increasing the temporal broadening. We find that a frequency resolution of 1 GHz can be achieved with less than -1300 ps/nm of dispersion by using a time-lens scheme. In contrast, the dispersion required using a single dispersive element to achieve the same frequency resolution is approximately 400,000 ps/nm, which is equivalent to approximately 23,000 km of standard SMF-28 fiber.

3. Experiment

The experimental setup for the spectral imaging system is shown in Fig. 2. The 1-nm bandwidth signal centered at 1536.14 nm, which is generated by filtering a broadband ASE source, is amplified and sent into an acetylene gas cell. The wavelength of the bandpass filter used to filter the broadband source is chosen such that the wavelength is centered on a single acetylene absorption line. An 80/20 coupler is used as a tap to monitor the absorption spectrum. The spectrum is measured using an optical spectrum analyzer (OSA) with a resolution of 0.01 nm. The 200-μW ASE signal imprinted with the absorption feature is sent into the first time-lens for frequency-to-time conversion [31]. In this time-lens, the signal is combined with a 1-nm bandwidth pump pulse with a peak power of approximately 100 mW, which has propagated

#107440 - $15.00 USD Received 10 Feb 2009; revised 20 Mar 2009; accepted 20 Mar 2009; published 25 Mar 2009

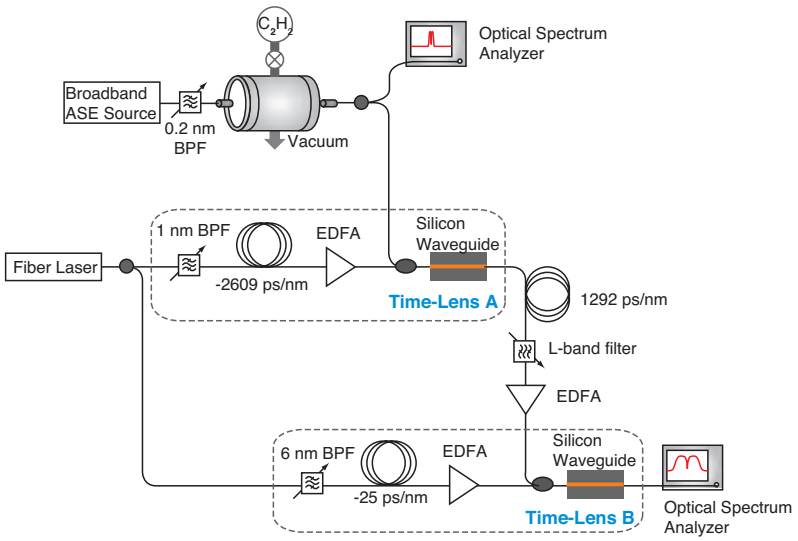

Fig. 2. Experimental setup of the spectral imaging system. The system consists of two FWM-based time-lenses, each with a different focal length.

through dispersion-compensating fiber (DCF) with a total dispersion of -2609 ps/nm, broadening the pulse from approximately 3.5 ps to 2.5 ns, and sent into a dispersion-tailored silicon waveguide for FWM wavelength conversion [32, 33]. Due to the pulsed pump, the FWM process temporally carves the input ASE signal. For a FWM-based time-lens, the focal length of the lens is equal to half the length of the dispersive fiber through which the pump pulse propagates. The signal is converted to the L-band, filtered, amplified, and sent through 70.2 km of SMF-28. This length is chosen to satisfy the lens equation for spectral magnification [Eq. (5)]. Finally, the signal is sent into the second time-lens for time-to-frequency conversion. Here, the signal is temporally overlapped with a 6-nm bandwidth pump pulse with a peak power of approximately 100 mW, which has propagated through a DCF with a total dispersion of -25 ps/nm, broadening the pulse from approximately 600 fs to 140 ps. FWM in the silicon waveguide converts the signal to 1543 nm, which we measure using an OSA. The power sensitivity of the system is approximately 100 μW and is limited by the FWM conversion efficiency in the silicon waveguide.

The experimental results are shown in Fig. 3. The plot shows the input spectrum (top) and the magnified spectrum after the spectral imaging system (bottom) for three different acetylene gas pressures. Comparing the input and the magnified spectrum, we achieve a magnification factor of 105. In addition, our frequency resolution matches that of the OSA we use to characterize our input, which indicates that our spectral imaging system has a resolution of 1 GHz. The noise in our output spectrum is due to the fact that the measured signal power is close to the sensitivity of our system. This can be improved by reducing the losses in the system and improving the FWM conversion efficiency. The center point of the spectral range can be adjusted by tuning the pump wavelength in the first time-lens to change the FWM wavelength shift, and by tuning the GDD imparted on the pump or the converted signal to satisfy the lens equation [Eq. (5)].

4. Discussion

The frequency resolution and the spectral range of the spectral imaging system are determined by the pump bandwidths and the dispersive lengths. The resolution is determined primarily by

#107440 - $15.00 USD Received 10 Feb 2009; revised 20 Mar 2009; accepted 20 Mar 2009; published 25 Mar 2009

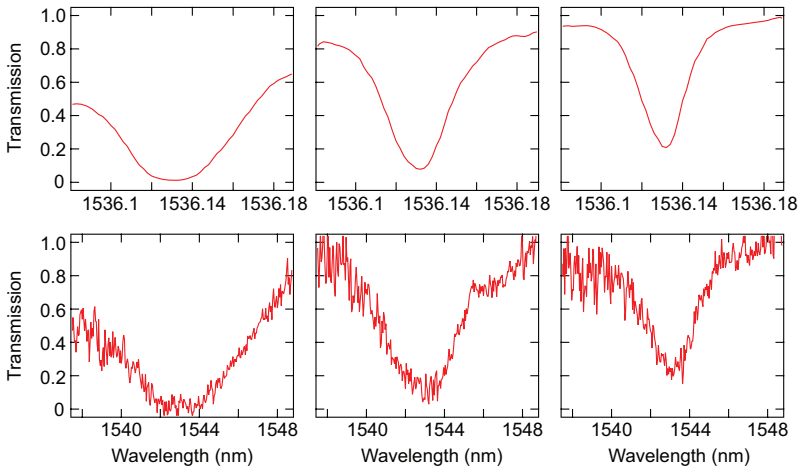

Fig. 3. Experimental results of the spectral imaging system. The plot shows the input (top) and the magnified output (bottom) for acetylene gas pressures of 600, 100, and 60 Torr (left to right). A frequency magnification factor of 105 is achieved.

the pump bandwidth of the first time-lens and the first dispersion length $\phi_A'' = \beta_2^{(A)} L^{(A)}$. For a single time-lens, the frequency-to-time conversion factor is [11],

$$\frac{\Delta\omega}{\Delta t} = -\frac{1}{\beta_2 L}. \tag{6}$$

The resolution of the imaging system can be determined from the frequency-to-time conversion of a spectral delta function in the first time-lens. The converted temporal pulsewidth is $\Delta\tau_{frequency-to-time} = \tau_p^{(A)}/\sqrt{2}$, where $\tau_p^{(A)}$ is the pump pulsewidth. Substituting this expression into Eq. (6), the frequency resolution is

$$\Delta\omega = -\frac{\tau_p^{(A)}}{\sqrt{2}\beta_2^{(A)} L_A}. \tag{7}$$

For our system, we predict a resolution of 0.22 GHz. Finer resolution can be achieved by using a broader pump bandwidth for the frequency-to-time conversion in the first time-lens. Practically, however, third-order dispersion (TOD) in the DCF in the time-lens and in the SMF used in the first focal length after the time-lens restricts the amount of bandwidth that can be utilized. To minimize the effect of TOD, the TOD dispersion length $L_{D3} = {T_0}^3/|\beta_3|$ must be larger than the length of the dispersive path used in the time-lens. Sub-500-MHz resolution can be achieved by using a low-TOD DCF [11], and the resolution can be further scaled by using a dispersion-flattened fiber.

The spectral range is determined by the pump bandwidth of the second lens and by the dispersive lengths. The maximum allowable temporal width for the time-to-frequency conversion is given by $\Delta T_{time-to-frequency} = 2\beta_2^{(B)} L_B \Omega_p^{(B)}$, where $\Omega_p^{(B)}$ is the pump bandwidth of the second time-lens. Substituting this into Eq. (6), the maximum spectral range is

$$\Delta\Omega = -\frac{2\beta_2^{(B)} L_B \Omega_p^{(B)}}{\beta_2^{(A)} L_A}. \tag{8}$$

For our system, we predict a spectral range of 14 GHz. The spectral measurement range can

#107440 - $15.00 USD Received 10 Feb 2009; revised 20 Mar 2009; accepted 20 Mar 2009; published 25 Mar 2009

be increased by using a broader pump bandwidth for the time-to-frequency conversion in the second time-lens. However, similar to the first time-lens, the pump bandwidth that ultimately can be utilized will be limited by TOD in the dispersive paths and the spectral profile of the pump pulse, which cause distortions in the quadratic phase shift of the time-lens.

5. Conclusion

In conclusion, we demonstrate a FWM time-lens based spectral imaging system with a 105$\times$ magnification factor and a 1-GHz frequency resolution. The pump wavelength can be tuned to adjust the four-wave mixing wavelength shift, allowing for a wide range of operating wavelengths. In addition, the imaging system can be configured for single-shot measurements. While conventional real-time spectrometers offer a large spectral measurement range, the resolution that can be achieved is limited. The imaging system offers potential as a tool for real-time, high resolution spectral diagnostics.

Acknowledgments

The authors thanks C. J. Hensley and O. Kuzucu for useful discussions. The authors also gratefully acknowledge support from DARPA through the arbitrary waveform generation program and the Center for Nanoscale Systems, supported by the NSF. This work was performed in part at the Cornell NanoScale Facility, a member of the National Nanotechnology Infrastructure Network, which is supported by the National Science Foundation (Grant ECS-0335765).

#107440 - $15.00 USD Received 10 Feb 2009; revised 20 Mar 2009; accepted 20 Mar 2009; published 25 Mar 2009